IEEE Transactions on Smart Grid, Volume 11, Issue 6, November 2020, pp. 4847-4859
DOI: 10.1109/TSG.2020.3003595

Mobile Emergency Generator Planning in Resilient Distribution Systems: A Three-Stage Stochastic Model with Nonanticipativity Constraints

Gang Zhang, Feng Zhang, *Member*, *IEEE*, Xin Zhang, *Senior Member*, *IEEE*, Zhaoyu Wang, *Member, IEEE*, Ke Meng, *Member*, *IEEE*, and Zhao Yang Dong, *Fellow*, *IEEE*

***Abstract*—Mobile emergency generators (MEGs) can effectively restore critical loads as flexible backup resources after power network disturbance from extreme events, thereby boosting the distribution system resilience. Therefore, MEGs are required to be optimally allocated and utilized. For this purpose, a novel three-stage stochastic planning model is proposed for MEG allocation of resilient distribution systems in consideration of planning stage (PLS), preventive response stage (PRS) and emergency response stage (ERS). Moreover, the nonanticipativity constraints are proposed to guarantee that the MEG allocation decisions are dependent on the stage-based uncertainties. Specifically, in the PLS, the intensity uncertainty (IU) of disasters and the outage uncertainty (OU) incurred by a given disaster are considered with probability-weighted scenarios for the effective MEG allocation. Then, with the IU that can be observed in the PRS, the MEGs are pre-positioned in the consideration of OU. It is noted that the pre-position decisions should only correspond to the IU realizations, according to nonanticipativity constraints. Last, with the further realization of OU in the ERS, the MEGs are re-routed from the pre-position to the target location, so that the provisional microgrids can be formed to restore critical loads. The proposed planning model can be large-scale due to multiple scenarios. Therefore, the progressive hedging algorithm (PHA) is customized to reduce the computational burden. The simulation results in 13 and 123 node distribution systems show the effectiveness and superiority of the proposed three-stage MEG planning model over the traditional two-stage model.**

***Index Terms*—Mobile generator planning, nonanticipativity constraints, distribution system, three-stage stochastic programming, resilience, uncertainty.**

ACRONYMS

ERS	Emergency response stage
IU	Intensity uncertainty
MEG	Mobile emergency generator
NBG	Non-black start distributed generator
NDM	Non-decomposition method
OU	Outage uncertainty
PHA	Progressive hedging algorithm
PLS	Planning stage
P-PHA	PHA with the parallelization technique
PRS	Preventive response stage
RTS	Restoration stage
RU	Repair time uncertainty

I. INTRODUCTION

Power distribution systems remain vulnerable to natural disasters due to the asset fragility, radial network topology, and limited back-up resources[1]. Disaster-induced disturbance can lead to multiple line outages in distribution networks, thereby threatening the security and continuity of electricity service to customers[2]. Therefore, it is important to take preventive measures to enhance the distribution network resilience against extreme events. Truck-mounted mobile emergency generators (MEGs) are considered as flexible and critical resources to restore the customers from power supply outages[3]. Specifically, MEGs can arrive at critical or isolated load points in two hours at speed of 80 kilometers per hour [4]. The mobility of MEGs can significantly reduce the outage duration of critical loads. Moreover, the energy capacity of MEGs can reach up to several MWh, and the MEGs can be re-fueled by the fuel trucks in case of long-lasting disaster events [5]. Hence, the continuous energy supply to critical loads can be guaranteed by the MEGs during the prolonged outage events. The enhanced mobility and large capacity enable the MEGs to be flexibly scheduled and dynamically dispatched according to the real-time conditions of post-disaster recovery process. Consequently, a feasible MEG planning strategy can effectively restore the critical loads and boost the distribution system resilience.

Generally, the distribution system resilience can be improved in 4 stages: planning stage (PLS), preventive response stage (PRS), emergency response stage (ERS) and restoration stage (RTS)[6]. In the PLS, the preventive measures on critical power assets can improve the network robustness and resource availability, such as the line hardening[7], overhead line vegetation management[8], backup generation allocation [9], and so on. In the PRS, emergency resources can be pre-allocated, and preventive operation strategies can be customized in preparation for the upcoming disaster events, such as the pre-position of the MEGs [10] and repair crews [11], and the proactive day-ahead scheduling methods [12] - [13]. In the ERS, critical loads can be restored by the real-time responsive strategies based on the available resources, such as the network configuration and provisional microgrid formation based on the MEGs [14] and other distributed energy resources such as battery storages [15]. In the

G. Zhang and F. Zhang are with the Key Laboratory of Power System Intelligent Dispatch and Control, Ministry of Education, Shandong University, Jinan, 250061, China (e-mail: fengzhang@sdu.edu.cn).

X. Zhang is with the Energy and Power Theme, School of Water, Energy and Environment, Cranfield University, Cranfield MK43 0AL, U.K. (e-mail:, xin.zhang@cranfield.ac.uk).

Z. Wang is with the Department of Electrical and Computer Engineering, Iowa State University, Ames, IA 50011 USA (e-mail: wzy@iastate.edu).

K. Meng and Z. Y. Dong are with the School of Electrical Engineering and Telecommunications, The University of New South Wales, NSW 2052, Australia (e-mail: kemeng@ieee.org, zydong@ieee.org).

© 2020 IEEE. Personal use of this material is permitted. Permission from IEEE must be obtained for all other uses, in any current or future media, including reprinting/republishing this material for advertising or promotional purposes, creating new collective works, for resale or redistribution to servers or lists, or reuse of any copyrighted component of this work in other works.

RTS, the maintenance crews are dispatched to repair the damaged facilities [16] - [17], and the distribution system can return to the normal condition step by step, which has been investigated elsewhere [18] and is not the main focus of this MEG planning paper. It can be seen that the planning decisions in PLS serve as the foundation of proactive measures in PRS and restoration strategies in ERS, while effective strategies in PRS and ERS can improve the efficiency of the planning resources, thereby reducing the generation investments. Consequently, the interdependence of PLS, PRS and ERS should be simultaneously taken into account, with a resilience-oriented planning model for MEG allocation, preventive operation and emergency response.

However, current studies mainly focused on the two-stage planning model for the allocation of emergency resources, i.e. the first stage of PLS to allocate preventive resources and the second stage of ERS to dispatch flexible resources. Specifically, references [7] and [8] proposed a two-stage robust and stochastic model respectively, in order to harden lines and allocate backup generators in PLS, and to minimize the load interruption costs in ERS. In [9], the decisions in PLS and ERS were coordinated in the two-stage robust programming in consideration of the spatial and temporal dynamics of an uncertain natural disaster. In [19], the two-stage robust model was adopted to harden components in PLS and dispatch generators in ERS in power transmission systems. In [20], the operational strategies of network reconfiguration and microgrid formation in ERS were integrated into the line hardening model in PLS to enhance the system resilience from the combined planning and operational perspectives by developing a two-stage model. In addition to the integration of PLS and ERS, the two-stage method has been employed in the synthetic model for combining proactive strategies in PRS with post-event re-dispatch in ERS. For example, in [6], the preventive and emergency responses of flexible generation were integrated in a two-stage robust model, with the first stage (i.e., PRS) to schedule the generators and the second stage (i.e., ERS) to update the scheduling and dispatch of generators to reduce the load curtailments. In [10], the MEGs were firstly pre-positioned in the PRS and then re-located to restore critical loads with a two-stage stochastic programming. In [12], a two-stage adaptive robust optimization was proposed to determine the unit commitment of generators and bids/offers in the day-ahead PRS, as well as the re-scheduling of generators, storage units, and elastic loads in the real time ERS to improve the resilience of a microgrid. In [21], a two-stage stochastic model was proposed to pre-allocate the repair crews in the PRS to reduce the outage restoration time in the ERS and enhance the system resilience. It can be seen that there is a research gap to formulate a three-stage stochastic model for MEG planning, preventive dispatch and emergency response to enhance the distribution system resilience.

The uncertainty at different stages of PLS, PRS and ERS is another critical factor affecting the MEG planning strategies [22]. Generally, based on the stage of uncertainty realization, the uncertainty to be considered in the resilience-oriented planning can be categorized to intensity uncertainty (IU) of different natural disasters and outage uncertainty (OU) incurred by a given natural disaster [23]. Specifically, IU denotes the random offensive resources of disaster events that the distribution system may encounter. It is noted that IU, e.g., hurricane force, can be predicted based on the sufficient situational awareness of a power grid in the PRS [6]. Then, OU represents the random outage incurred by a given natural disaster due to the nonlinear effect of the disaster to system components in the ERS. However, the two-stage method manages these uncertainties with no consideration of multi-uncertainties realization over stages, which leads to the ineffective utilization of available resources and sub-economic planning strategy.

In this paper, a novel stochastic model is proposed for the MEG planning in PLS, pre-position in PRS and real-time re-dispatch in ERS for the resilience enhancement in distribution systems. Moreover, the MEG planning and allocation decisions are integrated with multi-uncertainties (IU and OU) over three stages. Consequently, the future MEG decisions are adaptive to the stage-by-stage uncertainty realizations. The main contributions are presented as follows:

1) A novel three-stage stochastic programming model is proposed to allocate MEGs in distribution systems. By combining the planning strategy in PLS, pre-position decision in PRS and real-time dispatch in ERS, the MEGs can be effectively utilized across the three system resilience stages, thereby reducing the investment costs and enhancing the system resilience.

2) The proposed model considers the stage-by-stage uncertainty realization of IU and OU with nonanticipativity constraints, thereby achieving “dynamic” decision-making across different resilience stages instead of “unchanged” decisions in the two-stage model.

3) To solve the computational burden incurred by a large number of scenarios, an effective progressive hedging algorithm (PHA) is customized to decompose the original problem of three-stage stochastic model into several sub-problems with respect to different scenarios.

The remaining paper is organized as follows. Conceptual framework is described in Section II. Mathematical formulation is presented in Section III. Solution method is described in Section IV. Case studies are introduced in Section V, and the conclusion is drawn in Section VI.

II. Conceptual Framework

In this section, the conceptual framework of the proposed three-stage stochastic programming planning model for MEGs is proposed and compared with two-stage model, as shown in Fig.1. It is noted that a realization of IU is used to simulate the occurrence of a disaster event. Hence, a realization of IU can represent a disaster event in this paper. It is assumed that two disaster scenarios are considered as alternatives, i.e., IU1 and IU2 in Fig. 1, and they are independent of each other. Moreover, each disaster can cause 2 independent outage scenarios, termed as OU1-1, OU1-2, OU2-1 and OU2-2, respectively. Consequently, there are totally 4 scenarios, denoted as S1={IU1, OU1-1}, S2={IU1, OU1-2}, S3={IU2, OU2-1} and S4={IU2, OU2-2}, respectively. In the two-stage model, the MEG planning and pre-position decisions are made in PLS. Then, there is no proactive measure to be taken in the second stage of PRS by

considering the realization of IU, and thus the pre-event MEG locations remain unchanged. Last, with the realization of OU in ERS, the MEGs are dispatched to restore critical loads. Since the natural disaster events can be predicted several days ahead with more accurate information when approaching to real-time, the flexible MEGs can be pre-positioned at proper nodes ready for a specific outage scenario that is driven by the oncoming disaster event. However, such important generation pre-position is ignored in the two-stage model leading to the sub-optimal MEG planning and delay in system restoration. Therefore, the MEGs cannot be effectively utilized with the two-stage model (i.e., placed in the incorrect or less-critical nodes).

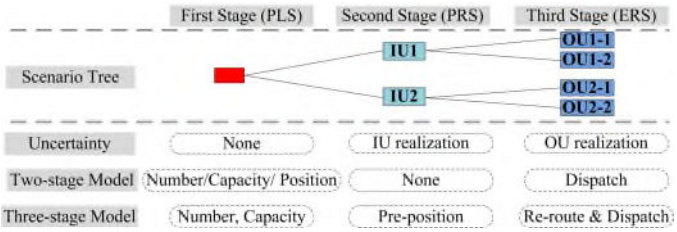


Fig.1 Comparison between two-stage and three-stage model

The proposed three-stage model makes the MEG decisions in each stage considering the future uncertainties with the multi-scenario based stochastic method. Moreover, the MEG decisions in each stage is related to the current realization of the respective uncertainty which is characterized by the nonanticipativity constraint. Comparing with the two-stage model, the current and future uncertainty information can be effectively utilized for the MEG planning and dispatch.

Specifically, in the PLS, the number and capacity of MEGs are firstly determined considering all possible scenarios (S1, S2, S3 and S4). However, since there is no uncertainty to be unfolded in the PLS, the planning decision in the PLS is dependent on no uncertainty.

Then, the MEGs can be pre-positioned in PRS for an efficient critical loads restoration in the ERS. The pre-position decision is dependent on the realization of the uncertainty in PRS, i.e., the IU realization (IU1 and IU2), which is characterized by the nonanticipativity constraint. Moreover, the future uncertainty of OU, is also considered in the pre-position strategy according to the stochastic method. For example, if the IU1 is determined in the PRS, the MEG pre-position will be made by considering the possible OU realizations of OU1-1 and OU1-2.

Last, with the further realization of OU (i.e., OU1-1, OU1-2, OU2-1 and OU2-2), the MEGs can be re-routed to appropriate locations and dispatched with the operational strategies of network reconfiguration and microgrid formation to reduce the load curtailments. It can be seen that MEGs are well utilized in both PRS and ERS to effectively enhance system resilience against disasters.

III. Mathematical Formulation

In this section, the mathematical formulation of the three-stage stochastic model for MEG planning is presented, including the PLS model in Section III-A, PRS model and nonanticipativity constraints in Section III-B, and ERS model in Section III-C.

A. MEG Planning in PLS

In the PLS, the MEGs with appropriate capacities are allocated with the consideration of IU and OU uncertainties. Hence, the objective (1) is to minimize the investment costs (the first term) and the expected penalty costs for the load interruption (the second term), by considering load priorities and load size. It is noted that the allocated MEGs in PLS are shared among all scenarios.

$$\min \sum_{k=1}^{K} C^g \cdot P_k^{cap} + \sum_{s\in S} \rho_s \cdot \sum_{i\in I} C^P \cdot w_i \cdot P_i^l \cdot T_{i,s}^{out} \tag{1}$$

$$\text{s.t. } x_k^{MEG} \cdot P^{umin,cap} \le P_k^{cap} \le x_k^{MEG} \cdot P^{umax,cap}, \quad \forall k \le K \tag{2}$$

$$\sum_{k=1}^{K} P_k^{cap} \le P^{tmax,cap} \tag{3}$$

where C^g represents the investment costs per capacity of MEGs; P_k^{cap} is the capacity of the allocated MEG k; ρ^s is the probability of scenario s; C^P is the penalty cost of unit load interruption; w_i is the priority of load i; $T_{i,s}^{out}$ is the outage duration of load i in scenario s; K is the maximum number of allocated MEGs; S is the set of scenarios, and I denotes the set of nodes in the distribution system. In addition to the limit on the number of MEGs, the unit capacity and total capacity are also constrained by the MEG technical restrictions and preventive investments for extreme events, as shown in (2) and (3), respectively, where x_k^{MEG} is the binary variable, which is 1 if the MEG k is decided to be allocated, and 0 otherwise; and $P^{umin,cap}$, $P^{umax,cap}$ and $P^{tmax,cap}$ are the MEG minimum unit capacity, maximum unit capacity and total capacity, respectively.

B. MEG Pre-position in PRS

Generally, the upcoming natural disasters, such as hurricanes, can be predicted with situational awareness a few days in advance with more accurate prediction when approaching to real-time. Therefore, the IU can be observed in PRS, such as IU1 or IU2 in Fig.1, and then corresponding proactive measures can be adopted in this stage to hedge against the expected disaster. In this paper, the allocated MEGs in PLS are strategically pre-positioned in PRS according to the IU realization. The MEGs can be flexibly re-routed to the target load bus, in preparation to reduce the outage duration and improve the distribution system resilience.

The binary variable $x_{k,i,s}^{pre}$ is employed to indicate whether the MEG k is pre-positioned at bus i in scenario s in PRS. The value of $x_{k,i,s}^{pre}$ is 1 if the MEG k is pre-positioned at bus i in scenario s, and 0 otherwise. The pre-position constraint (4a) ensures that each MEG is pre-positioned to only one location; (4b) indicates that each bus can be located with no more than one MEG; and (4c) indicates that only the MEG being allocated in PLS can be pre-positioned in PRS, and this constraint serves as the **MEG interrelation 1** between PLS and PRS.

$$\sum_{i\in I} x_{k,i,s}^{pre} \le 1, \forall k \le K, s \in S \tag{4a}$$

$$\sum_{k=1}^{K} x_{k,i,s}^{pre} \le 1, \forall i \in I, s \in S \tag{4}$$

b)

$$x_{k,i,s}^{pre} \le x_k^{MEG}, \forall k \le K, i \in I, s \in S \quad (4c)$$

It can be seen that $x_{k,i,s}^{pre}$ in the three-stage model is a "dynamic" and "wait to see" decision variable which keeps updating based on the realization of uncertainties of IU and OU. In comparison, the MEG pre-position decision in the two-stage model is indicated by the variable "$x_{k,i}^{pre}$", which remains unchanged with the gradually unfolded uncertainties over stages, thereby resulting in the less effective utilization of MEGs. Besides, the value of $x_{k,i,s}^{pre}$ should be dependent on the realization of IU, since the IU realization can be observed in the PRS. In this paper, the nonanticipativity constraints are proposed to characterize this feature.

First, the scenarios with the same IU realization can be classified into a specific set, denoted as $S'(IU)$. For this purpose, it is defined that IU_s^{PRS} and $IU_{s'}^{PRS}$ are the IU realizations in the scenario s and s', respectively. If $IU_s^{PRS} = IU_{s'}^{PRS} = IU$ is satisfied, both the scenario s and s' are classified into the set $S'(IU)$. Hence, for the scenario $s \in S'(IU)$ and $s' \in S'(IU)$, it is satisfied that $IU_s^{PRS} = IU_{s'}^{PRS} = IU$. Take the example in Fig. 2 for illustration, there are 4 scenarios (S1, S2, S3 and S4) and 2 IU realizations (IU1 and IU2). The scenario S1 and S2 share the same IU realization IU1, i.e., $IU_{S1}^{PRS} = IU_{S2}^{PRS} =$ IU1. Similarly, it can be obtained that $IU_{S3}^{PRS} = IU_{S4}^{PRS} =$ IU2. Hence, according to the above definition for $S'(IU)$, the scenarios S1 and S2 can be classified into the set S'(IU1), since $IU_{S1}^{PRS} = IU_{S2}^{PRS} =$ IU1. Similarly, the scenarios S3 and S4 can be classified into the set S'(IU2).

Then, when the IU realization is observed in the PRS, the MEG can be pre-positioned. In this case, the pre-position decisions in all scenarios with the same IU realization should be identical due to the same natural disaster effect. In other words, the scenarios belonging to the same set $S'(IU)$ should share one pre-position decision, as shown in (5). Moreover, the pre-position decision is dependent on the IU realization which can be observed in the current stage, hence the constraint (5) is defined as the nonanticipativity constraint.

$$x_{k,i,s}^{pre}(IU_s^{PRS}) = x_{k,i,s'}^{pre}(IU_{s'}^{PRS}), \forall S'(IU), \forall s, s' \in S'(IU), k \le K, i \in I \quad (5)$$

As shown in Fig. 2, the nonanticipativity constraint in (6) illustrates the S1 $\in S'$(IU1) and S2 $\in S'$(IU1), hence S1 and S2 should share the same pre-position decision. Similarly, the nonanticipativity constraint in (7) are applied for the scenario S3 and S4.

$$x_{k,i,S1}^{pre} = x_{k,i,S2}^{pre}, \forall k \le K, i \in I \quad (6)$$

$$x_{k,i,S3}^{pre} = x_{k,i,S4}^{pre}, \forall k \le K, i \in I \quad (7)$$

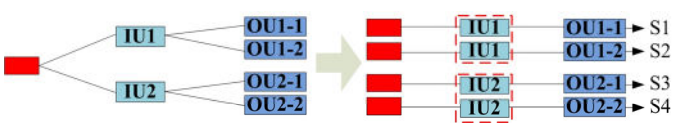


Fig.2 Illustration for nonanticipativity constraints

C. MEG real-time dispatch in ERS

With further realization of OU in ERS, the MEGs can be re-routed to the target locations to restore critical loads with operational strategies of network reconfiguration and microgrid formation. Comparing with other MEG real-time dispatch models such as in [10], the proposed model has innovative steps over 4 aspects of: 1) integrating the network reconfiguration (considering tie lines) and provisional microgrid formation with MEG dispatch to restore critical loads; 2) developing a single-commodity flow method to avoid the impractical assumption that all loads can be energized by the substations or MEGs after disaster; 3) avoiding a large number of binary variables to considerably reduce the computational burden; 4) enabling the participation of non-black start distributed generators (NBGs) in emergency response operation. Specifically, the proposed MEG real-time dispatch model comprises of the topology constraints (8)-(10), MEG re-routing model (11a)-(11c), energization status model (12)-(14), outage duration model (15)-(19), and operational constraints (20)-(25).

1) Topology Constraints

The distribution network and reformed microgrids are operated radially [24]. For this purpose, a single-commodity flow method is employed [20], with the requirements of: 1) the number of closed branches equals to the number of nodes minus the number of microgrids in (8); and 2) the connectivity in each microgrid is guaranteed by constraints in (9).

$$\sum_{(ij)\in B} v_{ij,s}^{f} = N_{bus} - \sum_{i \in I} v_{i,s}^{r}, \forall s \in S \quad (8)$$

$$\begin{cases} \sum_{j \in m(i)} F_{ij,s} - \sum_{j \in n(i)} F_{ji,s} \ge -1 - \mathrm{M} \cdot v_{i,s}^{r} \cdot (\sum_{k=1}^{K} x_{k,i,s}^{re} + v_{i,s}^{e}), \forall i \in I \\ \sum_{j \in m(i)} F_{ij,s} - \sum_{j \in n(i)} F_{ji,s} \le -1 + \mathrm{M} \cdot v_{i,s}^{r} \cdot (\sum_{k=1}^{K} x_{k,i,s}^{re} + v_{i,s}^{e}), \forall i \in I \\ -\mathrm{M} \cdot v_{ij,s}^{f} \le F_{ij,s} \le \mathrm{M} \cdot v_{ij,s}^{f}, \forall (ij) \in B \end{cases} \quad (9)$$

$$v_{ij,s}^{f} = v_{ij,s}^{w} \cdot z_{ij,s}, \forall (ij) \in B, s \in S \quad (10)$$

where $v_{ij,s}^{f}$ is the binary variable to represent the status of line ij in scenario s, the value is 1 if line ij is normally closed, and 0 otherwise, and it is determined by the damage status and switch status of line ij in scenario s, i.e., $z_{ij,s}$ and $v_{ij,s}^{w}$, as shown in (10); $F_{ij,s}$ is the fictitious flow of line ij in scenario s; $n(i)$ and $m(i)$ are the sets of all parent buses and children buses of bus i, respectively; M is a constant with the large value, which is used in the model formulation (Eq. 9 , 10, and 21) and the linearization method (Eq. 27). $v_{i,s}^{r}$ is the binary variable, the value is 1 if bus i is chosen as the root bus, and 0 otherwise; $x_{k,i,s}^{re}$ is the binary variable, the value is 1 if the MEG k is re-routed to bus i in scenario s, and 0 otherwise; $v_{i,s}^{e}$ is the binary parameter, the value is 1 if bus i is at either end of faulted lines in scenario s, and 0 otherwise.

2) MEG Re-routing Model in ERS

In the MEG re-routing model, each MEG is re-routed to exactly one location (11a); each bus can be located with no more than one MEG in ERS (11b) and only the MEG which have

been allocated in PLS can be re-routed in ERS (**MEG interrelation 2** between PLS and ERS) (11c).

$$\sum_{i\in I} x_{k,i,s}^{re} \le 1, \forall k \le K, s \in S \quad (11a)$$

$$\sum_{k=1}^{K} x_{k,i,s}^{re} \le 1, \forall i \in I, s \in S \quad (11b)$$

$$x_{k,i,s}^{re} \le x_k^{MEG}, \forall k \le K, i \in I, s \in S \quad (11c)$$

3) Energization Status Modeling

The constraints (12)-(13) are proposed to model the energization status of NBGs and loads. Specifically, a microgrid can be energized if and only if a black start generator, such as the MEG in this paper, is located at the root bus. To meet this requirement, binary variables $v_{i,s}^{a}$ are introduced, and the value is 1 if node i is connected to an energized microgrid in scenario s, and 0 otherwise. In other words, the available NBGs or loads at node i can be restored if $v_{i,s}^{a}=1$. Hence, the value of $v_{i,s}^{a}$ is bounded by constraints (12) and (13). The constraint (12) indicates that if node i is the root bus ($v_{i,s}^{r}=1$), the value of $v_{i,s}^{a}$ is determined by the value of $x_{k,i,s}^{re}$; if node i is not the root bus, the value of $v_{i,s}^{a}$ is determined by (13). In (13), if the final status of line ij is closed ($v_{ij,s}^{f}=1$), the value of $v_{i,s}^{a}$ equals to the value of $v_{j,s}^{a}$; if line ij is open with $v_{ij,s}^{f}=0$, the relationship between $v_{i,s}^{a}$ and $v_{j,s}^{a}$ is independent from each other therefore is not constrained by (13).

$$-1+v_{i,s}^{r}+\sum_{k=1}^{K} x_{k,i,s}^{re} \le v_{i,s}^{a} \le 1-v_{i,s}^{r}+\sum_{k=1}^{K} x_{k,i,s}^{re}, \forall i \in I, s \in S \quad (12)$$

$$-1+v_{ij,s}^{f}+v_{j,s}^{a} \le v_{i,s}^{a} \le 1-v_{ij,s}^{f}+v_{j,s}^{a}, \forall (ij) \in B, s \in S \quad (13)$$

In further, the binary variable $v_{i,s}^{L}$ is introduced to indicate that whether the loads at bus i are restored in scenario s. $v_{i,s}^{L}=1$ if the loads at bus i are restored in scenario s, and $v_{i,s}^{L}=0$ otherwise. Moreover, the loads at bus i can only be restored if bus i is energized, hence:

$$v_{i,s}^{L} \le v_{i,s}^{a}, \forall i \in I, s \in S \quad (14)$$

4) Outage Duration Modeling

First, the bus energization time is formulated to model the load outage duration. Specifically, for the nodes with MEGs, the energization time is equivalent to the time $T_{k,i,s}^{arr}$ when MEG k arrives at the bus i in scenario s as shown in (15). Moreover, $T_{k,i,s}^{arr}$ is determined by the MEG pre-position locations $x_{k,j,s}^{pre}$ and the travel time $T_{j,i}^{tra}$, which can be formulated in (16). It is noted that the constraint (16) represents the interrelation between the pre-position decisions in PRS and re-routing decisions in ERS (**MEG interrelation 3** between PRS and ERS).

$$\sum_{k=1}^{K}(x_{k,i,s}^{re}\cdot T_{k,i,s}^{arr}) \le t_{i,s}^{eng} \le \sum_{k=1}^{K}(x_{k,i,s}^{re}\cdot T_{k,i,s}^{arr})+(1-\sum_{k=1}^{K} x_{k,i,s}^{re})\cdot T^{rep}, \forall i \in I, s \in S \quad (15)$$

$$T_{k,i,s}^{arr}=\sum_{j\in I}(x_{k,j,s}^{pre}\cdot T_{j,i}^{tra})+(1-\sum_{j\in I} x_{k,j,s}^{pre})\cdot T^{rep}, \forall k \le K, i \in I, s \in S \quad (16)$$

where $t_{i,s}^{eng}$ is the energization time of bus i in scenario s; $T_{j,i}^{tra}$ is the travel time from bus j to bus i; and T^{rep} is the time when the damaged components are repaired and the system returns to normal conditions.

For the nodes which can be energized by microgrids, the energization time of one node is the same as other connected nodes ($v_{ij,s}^{f}=1$), as shown in (17)

$$v_{ij,s}^{f}\cdot t_{j,s}^{eng} \le t_{i,s}^{eng} \le v_{ij,s}^{f}\cdot t_{j,s}^{eng}+(1-v_{ij,s}^{f})\cdot T^{rep}, \forall (ij) \in B, s \in S \quad (17)$$

For the nodes which cannot be energized ($v_{i,s}^{a}=0$), the energization time is extended to the repair time of the damaged components T^{rep}, as shown in (18).

$$(1-v_{i,s}^{a})\cdot T^{rep} \le t_{i,s}^{eng} \le T^{rep}, \forall i \in I, s \in S \quad (18)$$

As shown in (19), $T_{i,s}^{out}$ represents the outage duration of the loads at bus i in scenario s, which is equivalent to the energization time of bus i if the loads are restored ($v_{i,s}^{L}=1$); Otherwise, the outage duration is dependent on the repair time T^{rep}.

$$T_{i,s}^{out}=v_{i,s}^{L}\cdot t_{i,s}^{eng}+(1-v_{i,s}^{L})\cdot T^{rep}, \forall i \in I, s \in S \quad (19)$$

5) Operational Constraints

Then, the operation of microgrids should meet certain technical constraints. In this paper, the linearized DistFlow model [25] is customized to model these constraints, and this method has been proved to be an effective measure in the resilient distribution system analysis [10], [20]. The following operational constraints are identified:

Equation (20) shows the real and reactive power balance of each node, where $P_{ij,s}$ and $Q_{ij,s}$ are active and reactive power flow through line ij in scenario s, respectively; $P_{k,i,s}^{MEG}$ and $Q_{k,i,s}^{MEG}$ are active and reactive power generation of the MEG k at node i in scenario s, respectively; $P_{i,s}^{NBG}$ and $Q_{i,s}^{NBG}$ are active and reactive power generation of the NBGs at node i in scenario s, respectively; ϕ^{L} is the power factor of the load.

$$\begin{cases} \sum_{j\in m(i)} P_{ij,s}-\sum_{j\in n(i)} P_{ji,s}=\sum_{k=1}^{K} P_{k,i,s}^{MEG}+P_{i,s}^{NBG}-v_{i,s}^{L}\cdot P_i^{L} \\ \sum_{j\in m(i)} Q_{ij,s}-\sum_{j\in n(i)} Q_{ji,s}=\sum_{k=1}^{K} Q_{k,i,s}^{MEG}+Q_{i,s}^{NBG}-v_{i,s}^{L}\cdot P_i^{L}\cdot\tan(\cos^{-1}(\phi^{L})) \end{cases}, \forall i \in I, s \in S \quad (20)$$

Equation (21) represents the voltage between the nodes connected by an energized branch ($v_{ij,s}^{f}=1$), where $U_{i,s}$ is the voltage amplitude at bus i in scenario s; R_{ij} and X_{ij} are the resistance and reactance of line ij, respectively; U_0 is the reference voltage.

$$\begin{cases} U_{i,s}-U_{j,s}-(R_{ij}P_{ij,s}+X_{ij}Q_{ij,s})/U_0 \le \mathrm{M}\cdot(1-v_{ij,s}^{f}) \\ U_{i,s}-U_{j,s}-(R_{ij}P_{ij,s}+X_{ij}Q_{ij,s})/U_0 \ge -\mathrm{M}\cdot(1-v_{ij,s}^{f}) \end{cases}, \forall (ij) \in B, s \in S \quad (21)$$

Constraint (22) defines the real and reactive power output of MEGs subject to the allocated capacity (P_k^{cap}) in PLS and the real-time location decision ($x_{k,i,s}^{re}$) (**MEG interrelation 4** between PLS and ERS). Constraint (23) defines the real and reactive power output of NBGs subject to the energization status of the connected node ($v_{i,s}^{a}$) and capacity ($P^{NBG,cap}$). It is noted that a NBG can be connected to the network only when the corresponding node is energized, i.e., $v_{i,s}^{a}=1$.

$$\begin{cases} 0 \le P_{k,i,s}^{MEG} \le x_{k,i,s}^{re}\cdot P_k^{cap} \\ 0 \le Q_{k,i,s}^{MEG} \le x_{k,i,s}^{re}\cdot Q_k^{cap} \end{cases}, \forall k \le K, i \in I, s \in S \quad (22)$$

2)

$$\begin{cases}0\le P_{i,s}^{NBG}\le v_{i,s}^{a}\cdot P^{NBG,cap}\\ 0\le Q_{i,s}^{NBG}\le v_{i,s}^{a}\cdot Q^{NBG,cap}\end{cases},\forall i\in I,s\in S \quad (2$$

3)

Constraint (24) limits the power flow through the closed and energized lines ($v_{ij,s}^{f}$=1), where P_{ij}^{max} and Q_{ij}^{max} are the active and reactive power transmission capacity of line *ij*. Constraint (25) limits the nodal voltage, where U_i^{max} and U_i^{min} are the maximum and minimum voltage magnitudes at bus *i*, respectively.

$$\begin{cases}-P_{ij}^{\max}\cdot v_{ij,s}^{f}\le P_{ij,s}\le P_{ij}^{\max}\cdot v_{ij,s}^{f}\\ -Q_{ij}^{\max}\cdot v_{ij,s}^{f}\le Q_{ij,s}\le Q_{ij}^{\max}\cdot v_{ij,s}^{f}\end{cases},\forall (ij)\in B,s\in S \quad (2$$

4)

$$U_i^{\min}\le U_{i,s}\le U_i^{\max},\forall i\in I,s\in S \quad (25)$$

Thus, the MEG planning problem is formulated as a three-stage stochastic non-linear model with nonanticipativity constraints. The allocated MEGs in PLS are assessed by the preposition decision in PRS and real-time dispatch in ERS with the stage-by-stage realizations of IU and OU.

6) Model Assumptions and Uncertainty Realization

The assumptions and uncertainty realization in the model formulation are discussed:

Disaster-related outage scenario generation with IU and OU realization. An intact disaster scenario is the combination of the IU realization and OU realization, such as S1={IU1, OU1-1} in Fig.2. Moreover, the disaster event with higher intensity can cause more severe outages. Hence, the IU and OU are highly interdependent. We propose the scenario generation method considering the interdependence of IU and OU as follows. First, possible realizations of IU can be generated with the statistical or simulation based model. For example, the IU can be modeled using the Weibull distribution [26], and the Monte Carlo techniques can be applied to generate the possible IU realizations [27]. Then, regarding to each IU realization, possible realizations of OU can be generated. Generally, the fragility curves are utilized to correlate the vulnerability of components to IU realizations as the relationship of IU and OU [28]. Subsequently, for each IU realization, the sampling method can be utilized to generate the values of OU. In this paper, we only provide the framework for the disaster scenario generation with no intention to investigate detailed sampling methods. Instead, we use the mature method in [29] to sample the outage scenarios by comparing the failure probability with the number sampling from the uniform distribution (0,1).

Repair time uncertainty. In this paper, the repair time is assumed to be deterministic. However, the repair time can be uncertain due to the random travel time of maintenance crews, the travel path, and the conditions of damaged equipment. Hence, the repair time uncertainty (RU) is highly dependent on the IU, and this characteristic is similar to the OU. The RU can also be considered in the three-stage model by following steps. First, the repair time uncertainty can be characterized with proper distributions, such as the lognormal distribution [30]. It is noted that the repair time is dependent on the weather conditions of IU realizations. Hence, the distribution of the repair time should be specific for a certain IU realization by a proper parameterization. Then, the proposed outage scenario generation method considering the interdependence of IU and (OU, RU) can be implemented. Since both the OU and RU can be observed in ERS, an intact scenario can be obtained by integrating the realizations of IU, OU and RU in the three-stage model. Other uncertainties, such as the demand uncertainty and the travel time uncertainty of MEGs, can be addressed with the same manner.

Energy capacity. It is assumed that the energy capacity of NBGs and MEGs can be sustained in the model, as the fuel supply to the MEGs and NBG can be guaranteed by several measures: 1) For the NBGs, the nodes with NBGs are generally equipped with the underground fuel storage tanks, and these tanks can be pre-filled in the PRS to extend the duration for the fuel supply in the ERS [31] [32]. Moreover, these fuel storage tanks can be re-filled by the fuel trucks in case of long-lasting disaster events. 2) The MEGs are generally equipped with the towable fuel tanks, which can provide the continuous fuel supply to the MEG for at least 24 hours [33]. Moreover, the accessibility should have been made available for the candidate nodes for MEG connection [34]. In this case, the system operators can strategically dispatch the fuel trucks to provide the sustainable fuel to MEGs in the ERS [35] [36]. By applying these methods, the sustainable fuel supply to the NBGs and MEGs can be ensured. Hence, the fuel supply and energy capacity are assumed to be sufficient in line with the previous studies [3] [37].

IV. Solution Method

It is a considerable challenge to solve this three-stage stochastic model due to the non-linearity and a large number of scenarios. In this paper, several linearization methods are adopted to linearize the three-stage model, and then a progressive hedging algorithm [38] is customized to decompose the original model to several scenario-based sub-problems, and substantially reduce the computational burden.

A. Linearization Method

The proposed model is nonlinear due to bilinear terms $v_{i,s}^{r}\cdot x_{k,i,s}^{re}$ in (9), $x_{k,i,s}^{re}\cdot T_{k,i,s}^{arr}$ in (15), $v_{ij,s}^{f}\cdot t_{i,s}^{eng}$ in (17), $v_{i,s}^{L}\cdot t_{i,s}^{eng}$ in (19), and $x_{k,i,s}^{re}\cdot P_k^{cap}$ in (22). These bilinear terms can be categorized into two types, i.e., the first type is to multiply two binary variables ($v_{i,s}^{r}\cdot x_{k,i,s}^{re}$) and the second type is to multiply the binary variable by continuous variable ($x_{k,i,s}^{re}\cdot T_{k,i,s}^{arr}$, $v_{ij,s}^{f}\cdot t_{i,s}^{eng}$, $v_{i,s}^{L}\cdot t_{i,s}^{eng}$, and $x_{k,i,s}^{re}\cdot P_k^{cap}$).

For the first-type bilinear term $v_{i,s}^{r}\cdot x_{k,i,s}^{re}$, we introduce an auxiliary binary variable $\alpha_{k,i,s}=v_{i,s}^{r}\cdot x_{k,i,s}^{re}$. Hence, $v_{i,s}^{r}\cdot x_{k,i,s}^{re}$ can be linearized as follows:

$$\alpha_{k,i,s}\le v_{i,s}^{r},\alpha_{k,i,s}\le x_{k,i,s}^{re},\alpha_{k,i,s}\ge v_{i,s}^{r}+x_{k,i,s}^{re}-1 \quad (2$$

6)

For the second-type bilinear term, take $x_{k,i,s}^{re}\cdot T_{k,i,s}^{arr}$ as an example, we introduce a continuous variable $\beta_{k,i,s}=x_{k,i,s}^{re}\cdot T_{k,i,s}^{arr}$. Hence, $x_{k,i,s}^{re}\cdot T_{k,i,s}^{arr}$ can be linearized as follows.

$$\begin{cases}-x_{k,i,s}^{re}\cdot \mathrm{M}\le\beta_{k,i,s}\le x_{k,i,s}^{re}\cdot \mathrm{M}\\ T_{k,i,s}^{arr}-(1-x_{k,i,s}^{re})\cdot \mathrm{M}\le\beta_{k,i,s}\le T_{k,i,s}^{arr}+(1-x_{k,i,s}^{re})\cdot \mathrm{M}\end{cases} \quad (27)$$

The above linearization methods can reform the original

MEG planning model to be solved as the linear problem. Then, the linear formulation of the MEG planning model is decomposed by the progressive hedging algorithm to reduce the computational burden.

B. Customized Progressive Hedging Algorithm

To illustrate the customized Progressive Hedging Algorithm (PHA), the linear formulation of the three-stage planning model is abbreviated as follows.

$$\min_{y^1,y_s^2,y_s^3} a^{\mathrm{T}}\cdot y^1+\sum_{s\in S}\rho_s\cdot(b_s^{\mathrm{T}}\cdot y_s^2+c_s^{\mathrm{T}}\cdot y_s^3) \tag{28}$$

$$\text{s.t. } A\cdot y^1+B_s\cdot y_s^2+C_s\cdot y_s^3\le d_s,\forall s\in S \tag{29}$$

$$y_s^2=y_{s'}^2,\ \forall S',\ \forall s,s'\in S' \tag{30}$$

where (28) represents the objective (1); (29) denotes all constraints excluding (5); (30) denotes the nonanticipativity constraint (5); y^1 is the planning decision in PLS; y_s^2 and y_s^3 are the pre-position and real-time dispatch decisions in PRS and ERS in scenario s, respectively. a, b_s, c_s and d_s are coefficient vectors, and A, B_s, and C_s are coefficient matrices.

It can be seen that multiple scenarios are coupled due to the PLS decision y^1 and the nonanticipativity constraint (30). Hence, the problem (28)-(30) can be reformulated as (31)-(32) by relaxing y^1 and (30) based on the PHA.

$$\min_{y_s^1,y_s^2,y_s^3}\sum_{s\in S}\rho_s\cdot\begin{bmatrix}a^{\mathrm{T}}\cdot y_s^1+b_s^{\mathrm{T}}\cdot y_s^2+c_s^{\mathrm{T}}\cdot y_s^3+(\lambda_s^{1,\mu})^{\mathrm{T}}\cdot y_s^1+(\lambda_s^{2,\mu})^{\mathrm{T}}\cdot y_s^2\\ +\eta/2\cdot\left\|y_s^1-\bar{y}_s^{1,\mu}\right\|^2+\eta/2\cdot\left\|y_s^2-\bar{y}_s^{2,\mu}\right\|^2\end{bmatrix} \tag{31}$$

$$\text{s.t. } A\cdot y_s^1+B_s\cdot y_s^2+C_s\cdot y_s^3\le d_s,\forall s\in S \tag{32}$$

where $\lambda_s^{1,\mu}$ and $\lambda_s^{2,\mu}$ are Lagrange-multiplier vectors concerning y^1 and (30) in the μ^{th} iteration of PHA; η is the penalty for $\left\|y_s^1-\bar{y}_s^{1,\mu}\right\|^2$ and $\left\|y_s^2-\bar{y}_s^{2,\mu}\right\|^2$; $\|\mathrm{g}\|^2$ represents the 2-norm; $\bar{y}_s^{1,\mu}$ and $\bar{y}_s^{2,\mu}$ are the probability-weighted average of current value of y_s^1 and y_s^2 in the μ^{th} iteration of PHA, respectively, and the formulations are shown in (33) and (34). The extended formulation of (33)-(34) is provided in Section Appendix-A.

$$\bar{y}_s^{1,\mu}=\sum_{s\in S}\rho_s\cdot y_s^{1,\mu},\forall s\in S \tag{33}$$

$$\bar{y}_s^{2,\mu}=\left(\sum_{s\in S'}\rho_s\cdot y_s^{2,\mu}\right)/\left(\sum_{s\in S'}\rho_s\right),\forall S',\ \forall s,\in S' \tag{34}$$

It can be seen that the formulation (31)-(32) is a scenario-decoupled problem, which can be decomposed to several sub-problems with respect to scenarios. Then, these scenario-based sub-problems can be solved in parallel to improve the computational efficiency. The steps of PHA to solve the three-stage model are outlined as follows.

Algorithm 1: Progressive Hedging Algorithm

1: Set the values for penalty η and convergence precision ε. Moreover, set iteration counter μ=0, Lagrange-multiplier vectors $\lambda_s^{1,\mu}=\lambda_s^{2,\mu}=0$, and $\bar{y}_s^{1,\mu}=\bar{y}_s^{2,\mu}=0$.

2. Solve (35)-(36) for all scenarios, and obtain the current optimal value of y_s^1 and y_s^2, denoted as $y_s^{1,\mu+1}$ and $y_s^{2,\mu+1}$, respectively. The extended formulation of (35)-(36) is provided in Section Appendix-B.

$$\min_{y_s^1,y_s^2,y_s^3}\ a^{\mathrm{T}}\cdot y_s^1+b_s^{\mathrm{T}}\cdot y_s^2+c_s^{\mathrm{T}}\cdot y_s^3+(\lambda_s^{1,\mu})^{\mathrm{T}}\cdot y_s^1+(\lambda_s^{2,\mu})^{\mathrm{T}}\cdot y_s^2 +\eta/2\cdot\left\|y_s^1-\bar{y}_s^{1,\mu}\right\|^2+\eta/2\cdot\left\|y_s^2-\bar{y}_s^{2,\mu}\right\|^2 \tag{35}$$

$$\text{s.t. } A\cdot y_s^1+B_s\cdot y_s^2+C_s\cdot y_s^3\le d_s \tag{36}$$

3. Calculate the value of $\bar{y}_s^{1,\mu+1}$ and $\bar{y}_s^{2,\mu+1}$ in (33)-(34).
4. Refine the value of $\lambda_s^{1,\mu+1}$ and $\lambda_s^{2,\mu+1}$ in (37).

$$\begin{cases}\lambda_s^{1,\mu+1}=\lambda_s^{1,\mu}+\eta\cdot(y_s^{1,\mu+1}-\bar{y}_s^{1,\mu+1})\\ \lambda_s^{2,\mu+1}=\lambda_s^{2,\mu}+\eta\cdot(y_s^{2,\mu+1}-\bar{y}_s^{2,\mu+1})\end{cases},\forall s\in S \tag{37}$$

5. If $\max\{\|y_s^{1,\mu+1}-\bar{y}_s^{1,\mu+1}\|,\|y_s^{2,\mu+1}-\bar{y}_s^{2,\mu+1}\|\}\le\varepsilon$, terminate; Else, set $\mu=\mu+1$, and repeat iteration from step 2.

In addition to the customized PHA, certain effective techniques can be applied to reduce the computational burden. First, scenario reduction methods can be employed to reduce the size of problem. The scenario reduction can be achieved by existing techniques or tailored rules[10] [39]. Then, the number of binary variables can be reduced by pre-processing methods. For example, the candidate nodes for MEG connection can be clustered by the principle of distance, thereby reducing the possible travel paths [37]. Last, some advanced computing methods can be utilized. For example, (31)-(32) can be decomposed to several sub-problems with respect to scenarios, hence the parallel solution method can be adopted to solve these scenario-based sub-problems. Moreover, the cloud computing method, which can solve the large-scale MILPs within seconds, can be employed for the large-size distribution system.

V. Case Study

In this section, case studies are performed in the modified IEEE 13-node and 123-node distribution systems. The 13-node system is used to validate the effectiveness and superiority of the three-stage planning model, while the larger 123-node system is to validate the computational efficiency of the solution method. All simulations are performed on GAMS 23.7/CPLEX 12.3 platform of a computer with a core i5, 3.2 GHz processor and 4 GB RAM.

A. Simulations on IEEE 13-node Distribution system

In this section, the simulations are performed based on a modified IEEE 13-node system as shown in Fig. 3. In particular, lines 4-9, 6-7 and 11-12 are added as normally open lines to form a meshed distribution system, these lines can be closed in the ERS for load restoration [40]. The total system loads are 1155.35kW, and the loads at nodes 4, 5 and 6 are critical loads with the priority coefficients of 2, 3 and 3, respectively. The candidate nodes for MEG connection are 3, 4, 5, 8, 11, 12, and 13, and these nodes can be selected based on the site, access and facility requirements [10]. It is assumed that two MEGs can be allocated in this system, and their capacities are bounded in

100~400kW due to the technical limits. The capital cost of MEGs is assumed to be $30/kW/year with 10-year life time [5], and the penalty cost for load curtailments is $14/kWh [41]. Moreover, the travel time between candidate nodes for MEG connection is 2~8h, and the reparation time of damaged components is set as 12h. In addition, NBG with capacity of 100kW is connected at node 13.

1) Demonstration of the three-stage model

A demonstration case with 3 IU realizations (i.e., IU-1, IU-2 and IU-3) and 9 scenarios (i.e., S1, S2, S3,⋯, S9) is utilized to illustrate the effectiveness of the proposed model, with one IU realization corresponding to three scenarios. The occurrence probability of three IU realizations is 0.3, 0.4 and 0.3, respectively, and the corresponding probability of 9 scenarios is 0.1, 0.1, 0.1, 0.133, 0.133, 0.133, 0.1, 0.1 and 0.1, respectively. The line outages and MEG decisions in PLS, PRS and ERS of each scenario are shown in Fig. 3.

In PLS, two MEGs are allocated with the capacity of 242.67kW (MEG 1) and 327.67kW (MEG 2) based on the proposed MEG planning model. Then, in PRS, the allocated MEGs in PLS are pre-positioned based on the respective IU realizations. For example, with the realization of IU-1, MEG 1 and MEG 2 are pre-located at node 5 and 12. It is noted that IU-1 realization is shared among scenarios S1, S2 and S3. Therefore, the MEG pre-position decisions should be identical in S1, S2 and S3 according to the nonanticipativity constraints (5), and are shown in Fig. 3 (S1, S2, and S3). Similar analysis can be conducted on other scenarios with different IU realizations. Moreover, the pre-position decision should be made in consideration of available MEGs, candidate nodes, load priority, MEG travel time and all possible OU realizations, so that the pre-positioned MEGs can be re-routed to the real-time location to reduce travel time and load outage duration.

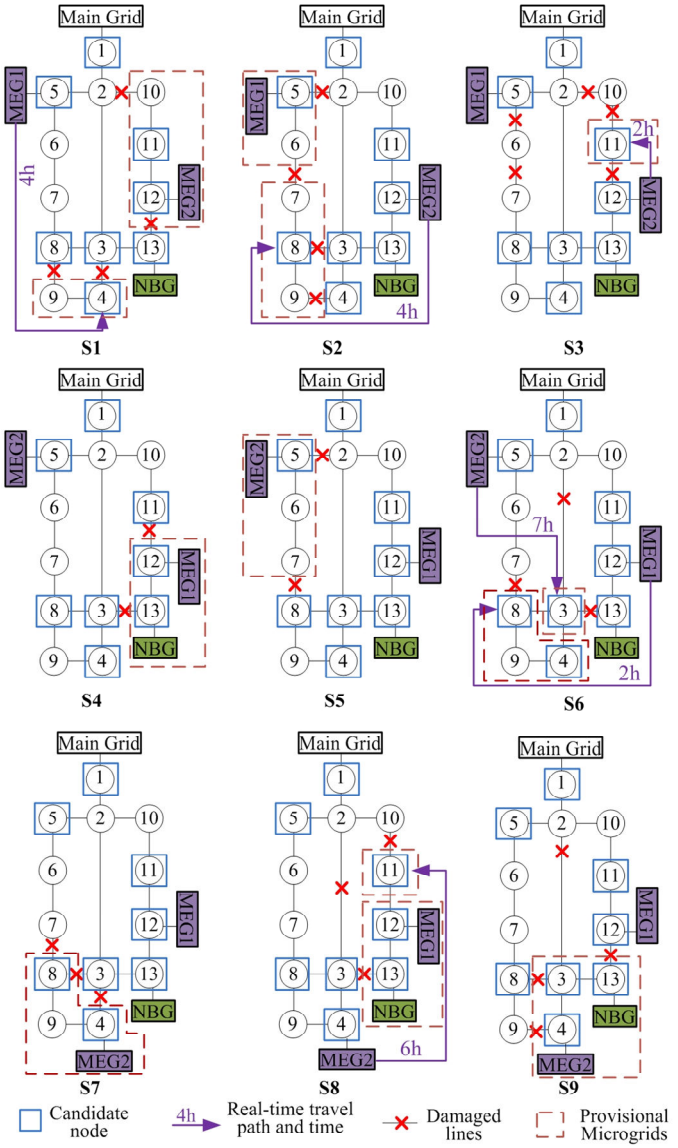


Fig.3 MEG decisions in PLS, PRS and ERS of scenario S1, S2, ⋯, S9 with microgrid reconfiguration

With the further realization of OU in ERS, certain lines are damaged in different scenarios as shown in Fig. 3. In each scenario, MEGs will be re-routed from the pre-position to the real-time locations, and operational strategies of system re-configuration and microgrid formation will be implemented to restore critical loads in ERS. For example, lines 2-10, 3-4, 8-9 and 2-10 are damaged in scenario S1. In this case, MEG1 is re-routed from node 5 to candidate node 4 to restore the loads at node 4 and 9 with the travel time of 4h, and MEG2 remains to be located at node 12 with no need for re-routing, this is due to the effective pre-position decisions in PRS considering the possible OU realizations. Moreover, the open lines 4-9, 6-7 and 11-12 are closed to form two provisional microgrids with MEG1 and MEG2 respectively. Therefore, the loads at node 4 and 9 can be restored in 4 hours, and the loads at node 10, 11 and 12 can be immediately restored with no delay by MEG travel time. Similar analysis can be conducted for other scenarios. It is noted that the ERS decisions are made in consideration of the system outages, MEG pre-position and capacities, load size, and MEG

travel time, which are considered in the proposed model.

In the ERS, NBGs serve as an important resource to jointly restore load in coordination with MEGs. For example, in scenario S8, MEG 1 with the capacity of 242.67kW is unable to restore the total loads of 337.67kW at nodes 12 and 13. However, MEG1 can energize the microgrid with node 13 where the 100kW NBG is located. Therefore, the loads at nodes 12 and 13 can be fully restored by the combination of MEG1 and NBG. In this case, the participation of NBGs can reduce the load curtailments and associated MEG investments.

It can be seen that the proposed three-stage model can effectively plan and dispatch MEGs by the pre-position strategy in PRS and re-routing decision in ERS, together with microgrid reformation and NBG coordination. The full-utilization of MEGs can effectively restore more loads and reduce load curtailment. The superiority of the proposed method will be justified in the next section by the comparison with other MEG planning methods.

In this paper, the penalty costs for load interruption are set to be \$14/kWh. However, load interruption costs can be up to \$57/kWh for some commercial customers in EU countries [42]. Hence, the sensitivity of the MEG planning decision to the load interruption cost is further investigated. For this purpose, the three-stage model is performed with the load interruption costs of \$4/kWh (*Case 1*), \$14/kWh (*Case 2*), and \$57/kWh (*Case 3*), respectively. Moreover, we have relaxed the constraints on the number of MEGs and the upper boundary of MEG power capacities. The simulation results are compared in Table I.

In Table I, the load interruption can be classified into three categories due to the different reasons for interruption as I1, I2 and I3 respectively. Specifically, I1 represents the load interruption which cannot be restored by MEGs or system reconfiguration, such as the load at node 3 in Fig. 3 (**S3**). Generally, the interruption duration of I1 is equivalent to the outage repair time. Then, I2 represents the load interruption that needs to be mitigated by MEG real-time dispatch, such as the load at node 11 in Fig. 3 (**S3**), therefore the interruption duration is equivalent to the travel time of MEGs. Last, I3 represents the load interruption due to the insufficient power generation capacity. For example, since the capacity of MEG2 (242.67kW) is insufficient to restore the total loads of 414.33kW at node 11 and 12 in Fig. 3 (**S1**), the loads at node 12 (281kW) have to be curtailed until the outage repair is completed.

It can be seen in Table I that higher load interruption costs tend to drive the three-stage model to allocate more MEGs with higher power capacities, thereby to minimize I2 and I3 load interruption. Specifically, by comparing between Case 1 and Case 2, it can be observed that the additional 476kW MEGs in Case 2 can reduce I2 load interruption by 2608 kWh and eliminate I3 load interruption to 0 kWh. Moreover, the travel time of MEGs in ERS can be shortened by pre-positioning more MEGs in PRS, thereby to help reduce the I2 load interruption. By comparing Case 2 and Case 3, the additional MEG power capacity of 57kW in Case 3 can further reduce I2 load interruption by 1189 kWh. These results indicate that the higher MEG capacity, the larger number of pre-positioned MEGs, and the proper dispatch strategy are effective to minimize the I2 and I3 load interruption, which are highly impacted by the costs of interrupted load.

TABLE I COMPARISON OF CASES WITH DIFFERENT INTERRUPTION COSTS

		Case 1	Case 2	Case 3
Power capacity (kW)		243	133+243+343	190+243+428
Total load interruption across 9 scenarios (kWh)	I1	920	920	920
	I2	5261	2653	1464
	I3	13584	0	0
	Total	19765	3573	2384

2) Superiority of the three-stage model

In this section, the proposed three-stage model is compared with the benchmark model (no MEG planning) and the two-stage model (no MEG pre-position or re-routing) to illustrate the superiority of the proposed model combining PLS, PRS and ERS with MEG pre-position, re-routing and real-time dispatch. First, the MEG investments and load curtailments for the three models are calculated in Table II.

TABLE II MEG INVESTMENTS AND LOAD INTERRUPTION IN THREE MODELS

		Benchmark	Two-stage	Three-stage
MEG Investments (\$/year)		0	20410	17560
Load interruption (kWh)	S1	7884	4512	2571
	S2	5192	1600	1197
	S3	2520	2520	1187
	S4	3372	0	0
	S5	2280	2280	0
	S6	5132	1700	1280
	S7	4112	1880	0
	S8	4972	3300	800
	S9	1700	2900	0
	Totally	37164	20692	7035
Objective value of Eq (1) (\$)		75693	69307	31516

Compared with the benchmark model, the objective value of \$44177 can be saved by the proposed three-stage model, which indicates the importance of MEG planning, pre-position and re-routing across the stages of PLS, PRS and ERS respectively. In further, the MEG investments of \$2850 can be saved with additional restoration of 13657kWh loads by comparing the proposed three-stage model with the two-stage. Therefore, the three-stage model demonstrates the superiority in reduced MEG investments and increased load restoration, due to the sufficient utilization of MEGs by pre-position in PRS and re-routing and dispatch of MEGs in ERS. In this paper, we employ the capacity utilization rate as evaluation index to justify the sufficient utilization of MEGs in the proposed three-stage model as shown in Table III. The capacity utilization rate is calculated as the ratio of utilized power capacity to the total capacity for each MEG.

TABLE III MEG CAPACITY UTILIZATION RATE OF TWO- AND THREE-STAGE MODEL

	Two-stage model		Three-stage model	
	MEG1 (%)	MEG2 (%)	MEG1 (%)	MEG2 (%)
S1	83	0	100	82
S2	0	87	55	87
S3	0	0	0	39
S4	100	0	98	0
S5	0	0	0	55
S6	0	100	35	100
S7	0	71	0	100
S8	100	0	98	39
S9	0	0	0	41
Average	32		50.6	

It can be seen that various line outage scenarios require different MEG utilization. The average MEG capacity utilization rate in three-stage model is 18.6 % higher than in the two-stage model. This is because the utilization of MEGs in the three-stage model can be improved by multiple strategies, such as the MEG pre-position for fast utilization of MEG, the real-time MEG re-routing for load energization, and the distribution system reconfiguration to energize microgrid by using MEGs. These strategies in the three-stage model can effectively utilize the planned MEGs, thereby reducing the MEG capacity investments as well as enhancing the distribution system resilience.

It is noted that not all MEGs are utilized in load restoration process across every scenario, such as MEG1 in scenario S3 is left unused for both models, and these MEGs may serve as the additional reserve for the unforeseen outages or to cover the failure risks of other MEGs. Generally, only limited scenarios can be entered in the MEG stochastic planning model due to the computational limitation. In this case, it is inevitable that some rare scenarios are unpredictable, thus being ignored in the planning model, and the outages caused by these scenarios are denoted as the "unforeseen outages". Although the unforeseen outages cannot be reflected for MEG planning and pre-position, the MEGs can be well utilized by the re-routing with the proposed operational model (38) when these unforeseen outages are observed in the ERS. For example, in scenario S3, MEG2 is re-routed from node 12 to node 11 to restore the load according to the simulation results of the planning model, and MEG1 can serve as the capacity reserve for the unforeseen outages. In this case, if an unforeseen outage occurs where line 3-13 is further damaged by disasters in scenario S3, MEG1 can be re-routed to node 13 to restore the isolated load 12 and 13 according to the model (38). It can be seen that the detrimental effect of the unforeseen outage can be alleviated by the reserve provided by MEG1. Moreover, the MEG reserve can also be utilized to accommodate the fluctuation of loads, and restore more loads if certain lines can be promptly repaired. For example, if line 3-4 can return to service early than scheduled in scenario S1, the loads at nodes 4 and 9 can be restored by the main grid, and MEG1 can be utilized to restore the load at node 11, since the capacity of MEG2 (242.67kW) is not sufficient to restore the total loads of 414.33kW at node 11 and 12.

$$\begin{cases} \min \sum_{i\in I} C^{P}\cdot w_i \cdot P_i^{l}\cdot T_{i,s}^{out} \\ \text{s.t.Constraints (8)-(25)} \qquad \forall s\in S^{uf} \\ x_k^{MEG}=x_k^{MEG*},\ P_k^{cap}=P_k^{cap*},\ x_{k,i,s}^{pre}=x_{k,i,s}^{pre*} \end{cases} \tag{38}$$

where S^{uf} is the set of the unforeseen outage; x_k^{MEG}, P_k^{cap}, and $x_{k,i,s}^{pre}$ are the MEG optimal planning and pre-position decisions of the proposed model.

B. Simulations in IEEE 123-node Distribution System

In this section, the proposed three-stage model and solution method are further implemented in the modified IEEE 123-node system [43]. Three MEGs are planned to be allocated to the 10 available candidate connection nodes. Moreover, 6 stationary NBGs, named as NBG1, NBG2, ⋯, NBG6, have been allocated in the distribution system with the capacities of 200kW, 80kW, 100kW, 120kW, 80kW and 60kW, respectively. IU realization of 3 disasters are considered, and 30 outage scenarios are generated with the sampling method in [10]. Based on these assumptions, the three-stage decisions in MEG planning, pre-position and re-routing are illustrated in Fig. 4.

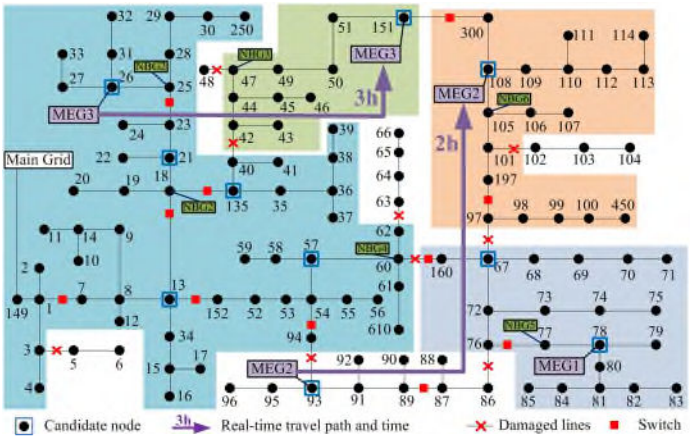


Fig.4 MEG decisions in PLS, PRS and ERS of an outage scenario in a 123-node distribution system.

In PLS, three MEGs are planned in the distribution system: MEG1, MEG2 and MEG3 with the capacities of 278kW, 276kW and 244kW, respectively. Then, with the realization of IU in PRS, three MEGs are pre-positioned to the candidate nodes 78, 93 and 26 ready for load restoration when outage scenario is observed in ERS. Last, 9 lines are damaged in ERS, and MEG2 and MEG3 are re-routed to node 108 and 151with the travel time of 2h and 3h, respectively, and two microgrids are formed to restore loads. Moreover, MEG1 remains at the pre-position location to immediately energize a microgrid with no time delay, this is due to effective pre-position strategy in PRS. The MEG capacity planning, pre-position, re-routing and microgrid formation across PLS, PRS and ERS demonstrate an improved system resilience by the proposed model.

Then, the proposed PHA to enhance the computational performance is compared with the non-decomposition method (NDM), as shown in Table IV. The NDM is incapable of generating a feasible solution for the proposed model within 12 hours if more than 6 scenarios are reached as shown in the last three rows of Table IV. In comparison, the PHA can converge for the 30-scenario case within the acceptable CPU time of 2 hours, and a high-quality solution with a small relative error of 4% can be obtained. Consequently, the proposed PHA method can effectively achieve feasible solutions for all outage scenarios in reasonable timescales, and can effectively reduce the computational burden by comparing with other NDM mothed.

Moreover, the scenario number has nonlinear effect on the CPU time for two reasons. First, the calculation time spent for solving (35)-(36) varies with simulation cases, and this difference is caused by the variable outage scenarios in these simulation cases as shown in Table V (Row 2). Moreover, even for a certain scenario in a certain simulation case, the calculation time spent for solving (35)-(36) can change from 3s to 792s with the iteration index due to the variable value calculation of $\lambda_s^{1,\mu}$, $\lambda_s^{2,\mu}$, $\bar{y}_s^{1,\mu}$ and $\bar{y}_s^{2,\mu}$ during the solution process, as shown in

Fig. 5. In this regard, the computational efficiency can be improved by advanced computing methods. For example, the problems (35)-(36) for different scenarios in a certain iteration can be solved in parallel. By applying the parallelization in the PHA (termed as P-PHA), the computation time can be reduced by up to 65% as shown in Table V (Row 6).

Second, the relationship between the scenario number and iteration number is also nonlinear, since the binary decision variables render the three-stage model non-convex and add nonlinear calculation time to the solution. However, the proposed PHA is able to converge within a reasonable number of iterations for solving the three-stage model as shown in Table V (Row 3). This finding has also been demonstrated in [44] by performing a class of stochastic mixed-integer problems. Moreover, the convergence performance can be further enhanced by some heuristic rules, such as the parameter modification and variable "fixing" strategy [44], which will be investigated as the future work.

TABLE IV COMPARISON OF PHA AND NDM

Number of scenarios	CPU time (Seconds)		Objective value of Eq (1) ($)		
	NDM	PHA	NDM/Optimal	PHA	Relative error
3	4	23	159198	165594	4.02%
6	1729	224	181437	188445	3.86%
9	N/A	527	N/A	212707	N/A
15	N/A	2209	N/A	238048	N/A
30	N/A	7254	N/A	239243	N/A

TABLE V COMPARISON OF PHA AND P-PHA

Scenario number	3	6	9	15	30
Average CPU time spent for each scenario in PHA (s)	1.53	4.14	5.85	4.91	4.09
Iteration number of PHA	5	9	10	30	59
CPU time of PHA (s)	23	224	527	2209	7254
CPU time of P-PHA (s)	12	114	199	1117	2518
CPU time reduced by P-PHA (%)	48%	49%	62%	49%	65%

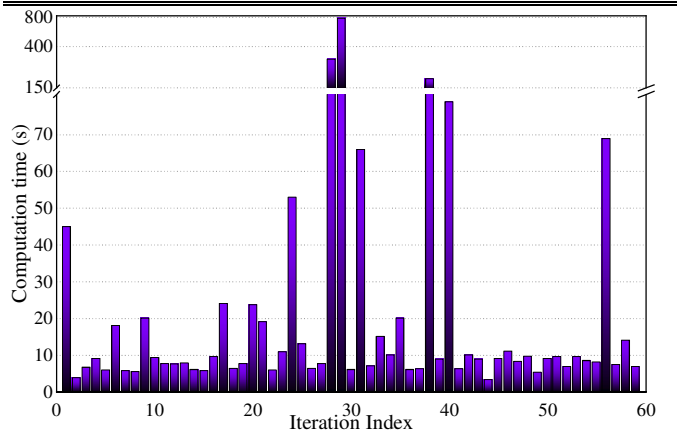


Fig. 5 The CPU time of (35)-(36) for a scenario in the 30-scenario case

VI. CONCLUSION

This paper proposes a MEG planning method to enhance the resilience of distribution systems against natural disasters. The planning method is realized by a three-stage stochastic framework with the capacity planning in PLS, the pre-position in PRS, and the real-time dispatch in ERS. Simulations in two IEEE distribution systems have validated the effectiveness of the proposed method in planning and dispatch MEG to improve the system resilience. In PLS, the MEG capacity planning method can optimally minimize the MEG investments and load interruption costs. In PRS, the planned MEGs can be pre-positioned at the proper candidate connection nodes in preparation for the oncoming disaster event, and substantially reduce the travel time of MEGs for load restoration. In ERS, the MEGs can be re-routed and dispatched to the re-configured microgrids to restore critical loads. Compared with the existing two-stage method, the proposed MEG planning and dispatch method can integrate the stage-by-stage uncertainty realization of IU and OU with nonanticipativity constraints, hence the MEG investments and load interruption can be simultaneously reduced. Moreover, the A customized PHA is proposed to decompose the large-scale nonlinear MEG model to multiple sub-problems with respect to various outage scenarios, which can significantly improve the computational efficiency of the solution method.

APPENDIX

A. Extended Formulation of (33)-(34)

The extended formulation of (33) and (34) is provided as Eq. (39) and Eq. (40), respectively.

$$\begin{cases} \bar{x}_{k,s}^{MEG,\mu} = \sum_{s\in S} \rho_s \cdot x_{k,s}^{MEG,\mu}, \forall s \in S \\ \bar{P}_{k,s}^{cap,\mu} = \sum_{s\in S} \rho_s \cdot P_{k,s}^{cap,\mu}, \forall s \in S \end{cases} \tag{39}$$

$$\bar{x}_{k,i,s}^{pre,\mu} = \left(\sum_{s\in S'} \rho_s \cdot x_{k,i,s}^{pre,\mu}\right) \Big/ \left(\sum_{s\in S'} \rho_s\right), \forall S',\ \forall s, \in S' \tag{40}$$

where $x_{k,s}^{MEG,\mu}$, $P_{k,s}^{cap,\mu}$ and $x_{k,i,s}^{pre,\mu}$ are the optimal solution of $x_{k,s}^{MEG}$, $P_{k,s}^{cap}$ and $x_{k,i,s}^{pre}$ generated from the μ^{th} iteration of PHA; $\bar{x}_{k,s}^{MEG,\mu}$, $\bar{P}_{k,s}^{cap,\mu}$, $\bar{x}_{k,i,s}^{pre,\mu}$ the probability-weighted average of $x_{k,s}^{MEG,\mu}$, $P_{k,s}^{cap,\mu}$ and $x_{k,i,s}^{pre,\mu}$. Moreover, $y_s^{1,\mu}$ in (33) corresponds to $\bar{x}_{k,s}^{MEG,\mu}$, $\bar{P}_{k,s}^{cap,\mu}$ in (39), and $y_s^{2,\mu}$ in (34) corresponds to $\bar{x}_{k,i,s}^{pre,\mu}$ in (40).

B. Extended Formulation of (35)-(36)

The extended formulation of (35) and (36) is provided as (41) and (42), respectively.

$$\min\left\{ \underbrace{\sum_{k=1}^{K} C^g \cdot P_{k,s}^{cap}}_{a^{\mathrm{T}}\cdot y_s^1 \text{ in (35)}} + \underbrace{\sum C^P \cdot w_i \cdot P_i^l \cdot T_{i,s}^{out}}_{c_s^{\mathrm{T}}\cdot y_s^3 \text{ in (35)}} + \underbrace{\sum_{k=1}^{K} \lambda_{k,s}^{1,\mu,x} \cdot x_{k,s}^{MEG}}_{(\lambda_s^{1,\mu})^{\mathrm{T}}\cdot y_s^1 \text{ in (35)}} + \sum_{k=1}^{K} \lambda_{k,s}^{1,\mu,p} \cdot P_{k,s}^{cap} \right.$$
$$+ \underbrace{\sum\sum \lambda_{k,i,s}^{2,\mu,x} \cdot x_{k,i,s}^{pre}}_{(\lambda_s^{2,\mu})^{\mathrm{T}}\cdot y_s^2 \text{ in (35)}} + \underbrace{\frac{\eta}{2}\left[\sum_{k=1}^{K} (x_{k,s}^{MEG} - \bar{x}_{k,s}^{MEG,\mu})^2 + \sum_{k=1}^{K} (P_{k,s}^{cap} - \bar{P}_{k,s}^{cap,\mu})^2\right]}_{\|y_s^1 - \bar{y}_s^{1,\mu}\|^2 \text{ in (35)}}$$
$$\left. + \underbrace{\frac{\eta}{2}\left[\sum\sum (x_{k,i,s}^{pre} - \bar{x}_{k,i,s}^{pre,\mu})^2\right]}_{\|y_s^2 - \bar{y}_s^{2,\mu}\|^2 \text{ in (35)}} \right\} \tag{41}$$

$$
\begin{aligned}
s.t.\ & 1)\textbf{PLS}\text{: Capacity constraints (2)–(3)} \\
& 2)\textbf{PRS}\text{: MEG pre-position constraints (4}a\text{)–(4}c\text{)} \\
& 3)\textbf{ERS}\text{: Topology constraints (8)–(10)} \\
& 4)\textbf{ERS}\text{: MEG re-routing model (11}a\text{)–(11}c\text{)} \\
& 5)\textbf{ERS}\text{: Energization status modeling (12)–(14)} \\
& 6)\textbf{ERS}\text{: Outage duration modeling (15)–(19)} \\
& 7)\textbf{ERS}\text{: Operational constraints (20)–(25)} \\
& 8)\text{The planning decision variables } x_k^{MEG}, P_k^{cap} \text{ are replaced} \\
& \quad \text{with the scenario-based } x_{k,s}^{MEG}, P_{k,s}^{cap} \text{ in all constraints.}
\end{aligned} \tag{42}
$$

REFERENCES

[1] G. Young, and J. Peters, "Synthetic structure of industrial plastics," *Plastics*, 2nd ed., vol. 3, J. Peters, Ed. New York, NY, USA: McGraw-Hill, 1964, pp. 15–64.

[2] C. Chen, J. Wang, and D. ton, "Modernizing Distribution System Restoration to Achieve Grid Resiliency Against Extreme Weather Events: An Integrated Solution," *Proc. IEEE,* vol. 105, no. 7, pp. 1267-1288, Jul.2017.

[3] J. Shang, X. Sheng, J. H. Zhang, and W. Zhao, "The optimized allocation of mobile emergency generator based on the loads importance," *Proc. Asia Pac. Power Energy Eng. Conf.*, pp. 1–4, Mar. 2009.

[4] "*Improving Electric Grid Reliability and Resilience: Lessons Learned From Superstorm Sandy and Other Extreme Events*," The GridWise Alliance. (2013). [Online]. Available: http://www.gridwise.org/documents/ImprovingElectricGridReliabilityandResilience_6_6_13webFINAL.pdf.

[5] L. Zhou, M. Fan, and Z. Zhang, "A study on the optimal allocation of emergency power supplies in urban electric network," in *Proc. 20th Int. Conf. Exhibit. Elect. Distrib.*, Jun. 2009, pp. 1-4.

[6] G. Huang, J. Wang, C. Chen, J. Qi, and C. Guo, "Integration of Preventive and Emergency Responses for Power Grid Resilience Enhancement," *IEEE Trans. Power Syst.,* vol. 32, no. 6, pp. 4451-4463, 2017.

[7] S. Ma, L. Su, Z. Wang, F. Qiu, and G. Guo, "Resilience Enhancement of Distribution Grids Against Extreme Weather Events," *IEEE Trans. Power Syst.,* vol. 33, no. 5, pp. 4842-4853, 2018.

[8] S. Ma, B. Chen, and Z. Wang, "Resilience Enhancement Strategy for Distribution Systems Under Extreme Weather Events," *IEEE Trans. Smart Grid,* vol. 9, no. 2, pp. 1442-1451, 2018.

[9] W. Yuan, J. Wang, F. Qiu, C. Chen, C. Kang, and B. Zeng, "Robust Optimization-Based Resilient Distribution Network Planning Against Natural Disasters," *IEEE Trans. Smart Grid,* vol. 7, no. 6, pp. 2817-2826, 2016.

[10] S. Lei, J. Wang, C. Chen, and Y. Hou, "Mobile Emergency Generator Pre-Positioning and Real-Time Allocation for Resilient Response to Natural Disasters," *IEEE Trans. Smart Grid,* vol. 9, no. 3, pp. 2030-2041, 2018.

[11] S. K. Masoud, and S. M. Sadegh, "Pre-hurricane optimal placement model of repair teams to improve distribution network resilience," *Electr. Power Syst. Res.,* vol. 165, pp. 1-8, 2018.

[12] A. Gholami, T. Shekari, and S. Grijalva, "Proactive Management of Microgrids for Resiliency Enhancement: An Adaptive Robust Approach," *IEEE Trans. Sustain. Energy,* vol. 10, no. 1, pp. 470-480, 2019.

[13] A. Khodaei, "Resiliency-Oriented Microgrid Optimal Scheduling," *IEEE Trans. Smart Grid,* vol. 5, no. 4, pp. 1584-1591, 2014.

[14] K. S. A. Sedzro, A. J. Lamadrid, and L. F. Zuluaga, "Allocation of Resources Using a Microgrid Formation Approach for Resilient Electric Grids," *IEEE Trans. Power Syst.,* vol. 33, no. 3, pp. 2633-2643, 2018.

[15] S. Yao, P. Wang, and T. Zhao, "Transportable Energy Storage for More Resilient Distribution Systems With Multiple Microgrids," *IEEE Trans. Smart Grid,* vol. 10, no. 3, pp. 3331-3341, 2019.

[16] Y. Tan, F. Qiu, A. K. Das, D. S. Kirschen, P. Arabshahi, and J. Wang, "Scheduling Post-Disaster Repairs in Electricity Distribution Networks," *IEEE Trans. Power Syst.,* vol. 34, no. 4, pp. 2611-2621, 2019.

[17] B. Chen, Z. Ye, C. Chen, J. Wang, T. Ding, and Z. Bie, "Toward a Synthetic Model for Distribution System Restoration and Crew Dispatch," *IEEE Trans. Power Syst.,* vol. 34, no. 3, pp. 2228-2239, 2019.

[18] G. Zhang, F. Zhang, X. Zhang, K. Meng, and Z. Y. Dong, "Sequential Disaster Recovery Model for Distribution Systems with Co-Optimization of Maintenance and Restoration Crew Dispatch," *IEEE Trans. Smart Grid*, pp. 1-1, 2020. doi: 10.1109/TSG.2020.2994111.

[19] N. Alguacil, A. Delgadillo, and J. M. Arroyo, "A trilevel programming approach for electric grid defense planning," *Comput. Oper. Res.,* vol. 41, no. 1, pp. 282-290, 2014.

[20] G. Zhang, F. Zhang, X. Zhang, Q. Wu, and K. Meng, "A multi-disaster-scenario distributionally robust planning model for enhancing the resilience of distribution systems," *Int. J. Electr. Power Energy Syst.,* vol. 122, pp. 106161, 2020.

[21] A. Arab, A. Khodaei, S. K. Khator, K. Ding, V. A. Emesih, and Z. Han, "Stochastic Pre-hurricane Restoration Planning for Electric Power Systems Infrastructure," *IEEE Trans. Smart Grid,* vol. 6, no. 2, pp. 1046-1054, 2015.

[22] M. A. Mohamed, T. Chen, W. Su, and T. Jin, "Proactive Resilience of Power Systems Against Natural Disasters: A Literature Review," *IEEE Access,* vol. 7, pp. 163778-163795, 2019.

[23] Y. Xiang, and L. Wang, "An Improved Defender–Attacker–Defender Model for Transmission Line Defense Considering Offensive Resource Uncertainties," *IEEE Trans. Smart Grid,* vol. 10, no. 3, pp. 2534-2546, 2019.

[24] C. Chen, J. Wang, F. Qiu, and D. Zhao, "Resilient Distribution System by Microgrids Formation After Natural Disasters," *IEEE Trans. Smart Grid,* vol. 7, no. 2, pp. 958-966, 2016.

[25] M. E. Baran, and F. F. Wu, "Network reconfiguration in distribution systems for loss reduction and load balancing," *IEEE Trans. Power Del.,* vol. 4, no. 2, pp. 1401-1407, 1989.

[26] A. M. Salman, and Y. Li, "Assessing Climate Change Impact on System Reliability of Power Distribution Systems Subjected to Hurricanes," *J. Infrastruct. Syst.,* vol. 23, no. 1, pp. 04016024, May 2016.

[27] J. Dupačová, G. Consigli, and S. W. Wallace, "Scenarios for Multistage Stochastic Programs," *Ann. Oper. Res.,* vol. 100, no. 1-4, pp. 25-53, 2000.

[28] Y. Hao, Z. Wei, Z. Jin, and B. A. C., "Resilience Assessment of Overhead Power Distribution Systems under Strong Winds for Hardening Prioritization," *ASCE-ASME Journal of Risk and Uncertainty in Engineering Systems, Part A: Civil Engineering,* vol. 4, no. 4, pp. 04018037, 2018.

[29] J. Winkler, L. Dueñas-Osorio, R. Stein, and D. Subramanian, "Performance assessment of topologically diverse power systems subjected to hurricane events," *Rel. Eng. Syst. Safety,* vol. 95, no. 4, pp. 323-336, Apr. 2012.

[30] C. J. Zapata, S. C. Silva, and O. L. Burbano, "Repair models of power distribution components," in *Proc. IEEE/PES Transm. and Distrib. Conf. and Expo.*, Latin America, Bogota, Colombia, Aug. 2008, pp. 1-6.

[31] C. R. Nightingale, "The Design of Mobile Engine Driven Generating Sets and their Role in the British Telecommunications Network," in *Proc. 5th Int. Telecom. Energy Conf.*, Tokyo, Japan, Oct. 1983, pp. 144-150.

[32] Federal Emergency Management Agency, *Mitigation Assessment Team Report: Hurricane Sandy in New Jersey and New York*, 2013. [Online].Available:https://www.fema.gov/media-library/assets/documents/85922].

[33] Global Power Supply Ltd., *Mobile Diesel Generators-Cummins 350 kW DFEG*. [Online]. Available:https://www.globalpwr.com/products-page/diesel-generators/cummins-350-kw-dfeg-3/.

[34] S. Iwai, T. Kono, M. Hashiwaki, and Y. Kawagoe, "Use of mobile engine generators as source of back-up power," in *Proc. IEEE 31st Int. Telecom. Energy Conf.*, Incheon, South Korea, Oct. 2009, pp. 1-6.

[35] W. Ng, S. Leung, J. Lam, and S. Pan, "Petrol delivery tanker assignment and routing: A case study in Hong Kong," *J. Oper. Res. Soc.,* vol. 59, no. 9, pp. 1191-1200, 09/01, Sep. 2008.

[36] G. G. Brown, C. J. Ellis, G. W. Graves, and D. Ronen, "Real-Time Wide Area Dispatch of Mobil Tank Trucks," *INFORMS Journal on Applied Analytics,* vol. 17, no. 1, pp. 107-120, Feb. 1987.

[37] S. Lei, C. Chen, Y. Li, and Y. Hou, "Resilient Disaster Recovery Logistics of Distribution Systems: Co-Optimize Service Restoration With Repair Crew and Mobile Power Source Dispatch," *IEEE Trans. Smart Grid,* vol. 10, no. 6, pp. 6187-6202, Feb. 2019.

[38] R. T. Rockafellar, and R. J.-B. Wets, "Scenarios and Policy Aggregation in Optimization Under Uncertainty," *Math. Oper. Res.,* vol. 16, no. 1, pp. 119-147, Nov. 1991.

[39] J. Dupaová, N. Grwe-Kuska, and W. Rmisch, "Scenario reduction in stochastic programming," *Math. Program.,* vol. 95, no. 3, pp. 493-511, 2003.

[40] X. Wang, Z. Li, M. Shahidehpour, and C. Jiang, "Robust Line Hardening Strategies for Improving the Resilience of Distribution Systems With Variable Renewable Resources," *IEEE Trans. Sustain. Energy,* vol. 10, no. 1, pp. 386-395, 2019.

[41] P. Dehghanian, S. Aslan, and P. Dehghanian, "Maintaining Electric System Safety Through An Enhanced Network Resilience," *IEEE Trans. Ind. Appl.,* vol. 54, no. 5, pp. 4927-4937, 2018.
[42] M. Lehtonen, N. Gűndűz, and S. Küfeoğlu, "On the Evaluation of Customers Interruption Costs due to Unexpected Power Outages," *IEEE Annu. Int. Sci. Conf. Power Electr. Eng. Riga Tech. Univ., RTUCON - Proc*, pp. 1-4, 2018.
[43] B. Chen, Z. Ye, C. Chen, and J. Wang, "Toward a MILP Modeling Framework for Distribution System Restoration," *IEEE Trans. Power Syst.,* vol. 34, no. 3, pp. 1749-1760, 2019.
[44] J.-P. Watson, and D. L. Woodruff, "Progressive hedging innovations for a class of stochastic mixed-integer resource allocation problems," *Comput. Manag. Sci.,* vol. 8, no. 4, pp. 355-370, 2011.

Gang Zhang (S'18) received the B.Sc. degree in electrical engineering in 2016 from Shandong University, Jinan, China, where he is currently working toward the Ph.D. degree. His research interests include power system resilience and distribution system planning.

Feng Zhang (M'11) received his Ph.D. degree from Shandong University, China, in 2011. He is currently an Associate Professor in School of Electrical Engineering, Shandong University, Jinan, China. His research interests include renewable energy and energy storage.

Xin Zhang (M'16, SM'19) received the M.Sc. and Ph.D. degrees in electrical power engineering from The University of Manchester, U.K., in 2007 and 2010 respectively. He is an Associate Professor (Senior Lecturer) in energy systems at Cranfield University, U.K. His research and industrial experience include power system planning and operation.
.

Zhaoyu Wang (M'15) received the M.S. and Ph.D. degrees in electrical and computer engineering from the Georgia Institute of Technology in 2012 and 2015, respectively. He is the Harpole-Pentair Assistant Professor with Iowa State University. His research interests include power distribution systems and power system resilience.

Ke Meng (M'10, SM'19) received the Ph.D. degree in electrical engineering from the University of Queensland, Brisbane, QLD, Australia, in 2009. He is currently a Senior Lecturer with the School of Electrical Engineering and Telecommunications, The University of New South Wales, Sydney, NSW, Australia. His research interests include power system stability analysis, and wind power and energy storage.

Zhao Yang Dong (M'99–SM'06–F'17) received the Ph.D. degree from the University of Sydney, Sydney, Australia, in 1999. He is currently the SHARP Professor with the University of New South Wales, the Director of ARC Research Hub for Integrated Energy Storage Solutions, and the Director of UNSW Digital Grid Futures Institute, Sydney, NSW, Australia. His research interests include smart grid and power system planning.



https://dspace.org/

Mobile emergency generator planning in resilient distribution systems: a three-stage stochastic model with nonanticipativity constraints

Zhang, Gang; Zhang, Feng; Zhang, Xin; Wang, Zhaoyu; Meng, Ke ...

2020-06-19
IEEE
https://doi.org/10.1109/TSG.2020.3003595
Zhang G, Zhang F, Zhang X. et al., (2020) Mobile emergency generator planning in resilient distribution systems: a three-stage stochastic model with nonanticipativity constraints. IEEE Transactions on Smart Grid, Volume 11, Issue 6, November 2020, pp. 4847-4859

Downloaded from a DSpace repository. https://dspace.org/